

Case report

# An autopsy case of acute myocarditis with unique lymph node findings characterized by the proliferation of reactive plasmablasts

Haruo Ohtani,<sup>1,3)</sup> Yoshihiro Nozaki,<sup>2)</sup> Takashi Murakami,<sup>2)</sup> Lisheng Lin,<sup>2)</sup> Junko Shiono,<sup>2)</sup> Masaaki Miyazawa<sup>4)</sup>

We report an autopsy case of acute myocarditis, in which the mediastinal lymph nodes exhibited unique findings. A 15-year-old Japanese boy was diagnosed with the secondary onset of acute myocarditis. No viruses were identified. Autopsy confirmed acute lymphocytic myocarditis. Lymphadenopathy was observed, especially in pulmonary hilar/mediastinal areas. Microscopically, interfollicular areas were uniformly filled with medium-sized, round cells that resembled lymphocytes. They were immunohistochemically CD3<sup>-</sup> CD5<sup>-</sup> CD19<sup>+</sup> CD20<sup>-</sup> CD79a<sup>-</sup> Pax-5<sup>-</sup> CD138<sup>+</sup> MUM1<sup>+</sup> LMP1<sup>-</sup> EBNA2<sup>-</sup> cytoplasmic IgG<sup>+</sup> IgA<sup>-</sup> and IgM<sup>+</sup>. No monotypia was observed for kappa and lambda light chains, and multiplex polymerase chain reaction analyses of immunoglobulin heavy chain variable region diversity demonstrated oligoclonal peaks, suggesting reactive change. IgG<sup>+</sup> or VS38c<sup>+</sup> cells frequently co-expressed Ki-67 (up to 80%). We considered these cells abundantly present in lymph nodes to be reactive plasmablasts because they were early plasma cells with proliferative activity.

**Keywords:** plasmablasts, reactive lymphadenopathy, double-labeling immunohistochemistry

## INTRODUCTION

We report an autopsy case of acute myocarditis, in which pulmonary hilar/mediastinal lymph nodes exhibited proliferation of round cells that were judged to be reactive plasmablasts. As reactive plasmablasts have not been described in detail in the field of pathology, we describe the histological and molecular features of the lymph nodes, and discuss the significance of this lesion.

## CASE PRESENTATION

A 15-year-old Japanese boy developed fever 12 days prior to death. He was admitted to Ibaraki Children's Hospital 10 days prior to death due to dyspnea, vomiting, and continued fever. Electrocardiography revealed atrioventricular dissociation, ventricular escaped beats, and multifocal ventricular extrasystole without typical ischemic ST changes, and his echocardiogram demonstrated a decrease in left ventricular contractility. High serum creatine kinase was observed (3,514 IU/L [normal range 62-287]), which later increased to 35,056 IU/L. The patient was diagnosed with


acute myocarditis. He had a past history of acute myocarditis at the age of 12, which was treated at the same hospital with complete recovery; therefore, this was considered the secondary onset of the disease. The patient was started on extracorporeal membrane oxygenation (ECMO) 8 days prior to death. However, no recovery was observed. Virus infection is frequently associated with acute lymphocytic myocarditis,<sup>1,2</sup> but no viruses were identified from the patient at either onset of myocarditis (Table S1). Autopsy, performed 5 hours postmortem, confirmed the diagnosis of acute lymphocytic myocarditis: the heart, weighing 272 g, exhibited multifocal infiltration of lymphocytes, including both T- and B-lymphocytes, where degeneration and/or necrosis of myocardial cells was prominent (Fig. S1A-D). Scarring was observed only in the atrioventricular node (Fig. S1E). The lungs, weighing 976 g (left) and 1,092 g (right), exhibited diffuse alveolar hemorrhage (Fig. S2A, B).

Lymphadenopathy was marked in pulmonary hilar and mediastinal regions. The largest was in the right pulmonary hilar area of 2 cm in size. Microscopically, enlarged lymph nodes sampled from the pulmonary hilar area had the following features (Fig. 1A): 1) expansion of interfollicular areas,

Received: June 2, 2020. Revised: July 14, 2020. Accepted: July 27, 2020. Online Published: September 25, 2020 DOI:10.3960/jslrt.20023

<sup>1)</sup>Department of Pathology, Ibaraki Children's Hospital, Mito, Japan, <sup>2)</sup>Department of Pediatric Cardiology, Ibaraki Children's Hospital, Mito, Japan, <sup>3)</sup>Department of Pathology, Mito Saiseikai General Hospital, Mito, Japan, <sup>4)</sup>Department of Immunology, Kindai University Faculty of Medicine, Osaka-Sayama, Japan

**Corresponding author:** Haruo Ohtani, M.D., Department of Pathology, Ibaraki Children's Hospital, 3-3-1 Futabadai, Mito, 311-4145 Japan. E-mail: 311serenity@gmail.com  
Copyright © 2020 The Japanese Society for Lymphoreticular Tissue Research

 This work is licensed under a Creative Commons Attribution-NonCommercial-ShareAlike 4.0 International License.

2) no increase in germinal centers, and 3) vascular transformation of lymphatic sinuses. The basic architecture of lymph nodes was preserved. Retroperitoneal or mesenteric lymph nodes demonstrated no notable microscopic changes (Fig. 1B). Higher magnification in pulmonary hilar nodes revealed that interfollicular areas were filled with diffuse proliferation of round cells with scant amphophilic cytoplasm, which were larger (up to two-times) than small lymphocytes (Fig. 1C, D, Fig. S3). They occasionally had one or two prominent nucleoli. These cells were later identified as plasmablasts for the reasons described below. Typical plasma cells were hardly observed. Neutrophils were sporadically observed among round cells. The above morphological findings suggested T cell responses (*i.e.*, paracortical hyperplasia) caused by infection of unidentified organisms. However, the immunohistochemical results were unexpected: most round cells in the interfollicular areas were CD3<sup>-</sup> CD5<sup>-</sup> CD19<sup>+</sup> CD20<sup>-</sup> CD79a<sup>-</sup> Pax-5<sup>-</sup> CD138<sup>+</sup> (up to 50%), MUM1<sup>+</sup>, LMP1<sup>-</sup>, EBNA2<sup>-</sup>, and cytoplasmic IgG<sup>+</sup> IgA<sup>-</sup>, and IgM<sup>-</sup> (Fig. 2A-D, Fig. S4A-D). Kappa and lambda light chain staining did not demonstrate monotypia (Fig. 2E, F). As Ki-67<sup>+</sup> cells were abundant in this area, we performed double staining. First, we confirmed that neither CD3<sup>+</sup> T nor CD20<sup>+</sup> B cells in the expanded interfollicular area correspond to Ki-67<sup>+</sup> cells

(Fig. 3A, Fig. S5A). In sharp contrast, immunofluorescence staining revealed that both cytoplasmic IgG<sup>+</sup> cells and VS38c<sup>+</sup> cells frequently co-expressed Ki-67 (78% among IgG<sup>+</sup> cells) (Fig. 3B, C). Monoclonal antibody VS38c, which recognizes rough endoplasmic reticulum, is a marker of plasma cell differentiation among lymphoid cells.<sup>3</sup> Based on the staining results, the cytoplasmic IgG-positive round cells were considered to have significant proliferative activity. These cells corresponded to plasmablasts based on the definition used mainly in the immunology field because plasmablasts are defined as early plasma cells that have proliferative and/or migratory activity.<sup>4-6</sup>

To exclude the possibility of neoplastic changes, genomic DNA was extracted from the formalin-fixed, paraffin-embedded sections of pulmonary lymph nodes and junctional diversity of the immunoglobulin heavy chain variable regions was analyzed according to the standardized multiplex PCR protocol.<sup>7</sup> Amplification with the FR3-JH primer set yielded several distinct peaks embedded within a polyclonal background (Fig. S6A), whereas no monoclonal peak was observed with any of the used primer sets, including DH1-6-JH (Fig. S6B). This suggested that the plasmablast expansion was oligoclonal in nature.

Lymph nodes in other regions of the body (*i.e.*,

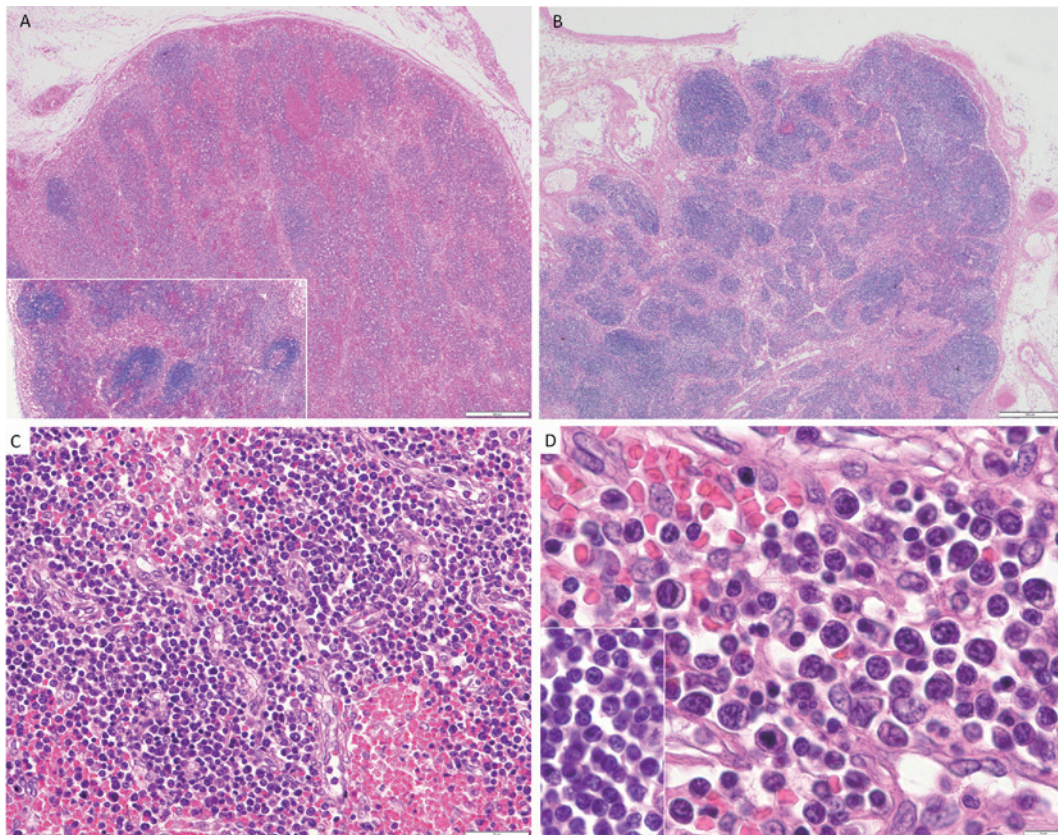


**Fig. 1.** HE staining of lymph nodes. **A)** Pulmonary hilar lymph node. Note expansion of extrafollicular areas. Lymph follicles are not abundant and only focally observed (inset). **B)** Retroperitoneal lymph node as a control. **C)** Mid-power and **D)** high-power views of the extrafollicular area of the pulmonary hilar lymph node, showing proliferation of round cells (plasmablasts). Inset in **D)** shows small lymphocytes observed in the paracortex of pulmonary hilar lymph nodes as size controls at the same magnification. Scales: 500  $\mu$ m (**A, B**), 50  $\mu$ m (**C**), and 10  $\mu$ m (**D** including the inset).

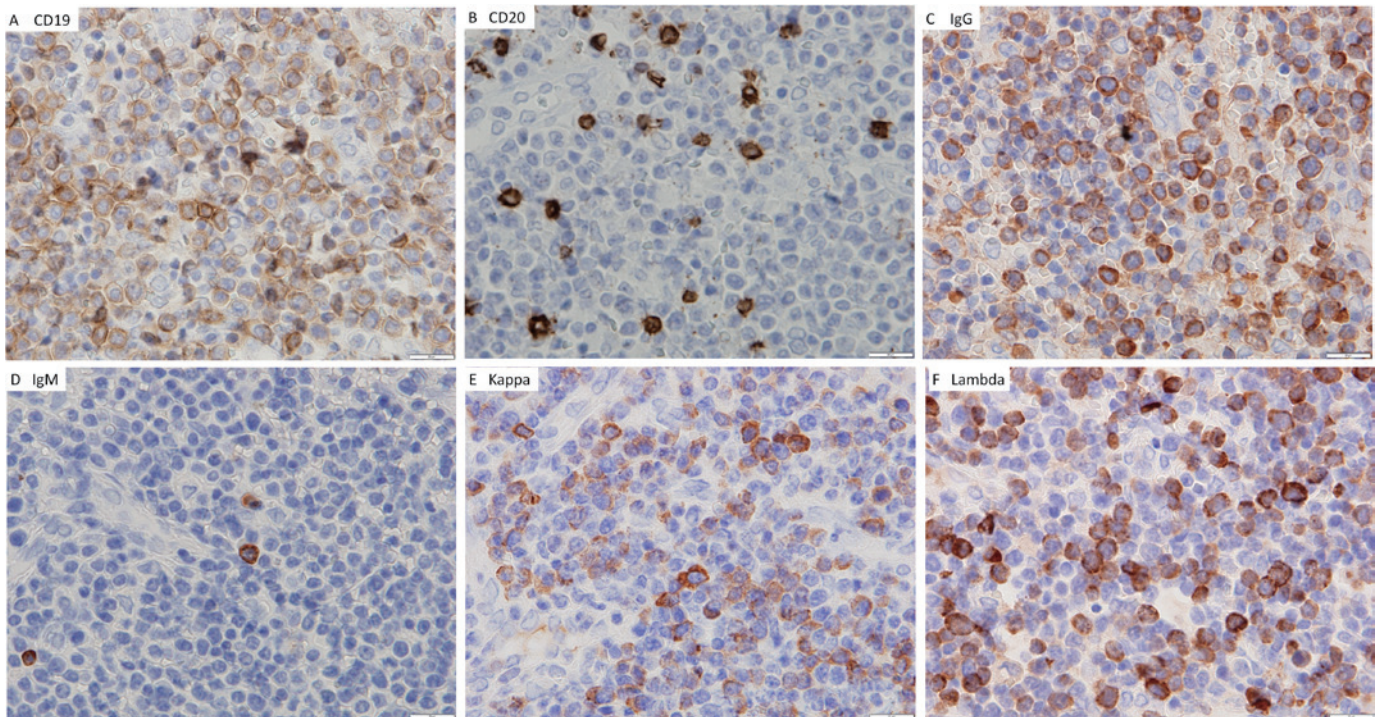


**Fig. 2.** Immunohistochemistry for round cells (plasmablasts) in the extrafollicular areas of the pulmonary hilar nodes, labeled by antibodies against *A*) CD19, *B*) CD20, *C*) IgG, *D*) IgM, *E*) kappa chain, and *F*) lambda chain. Plasmablasts are CD19<sup>+</sup> CD20<sup>-</sup> IgG<sup>+</sup> IgM<sup>-</sup>. Sparse CD20<sup>+</sup> cells were judged to be reactive B cells. No monotypia was observed for kappa and lambda chains. Scales: 20  $\mu$ m (*A-D*).

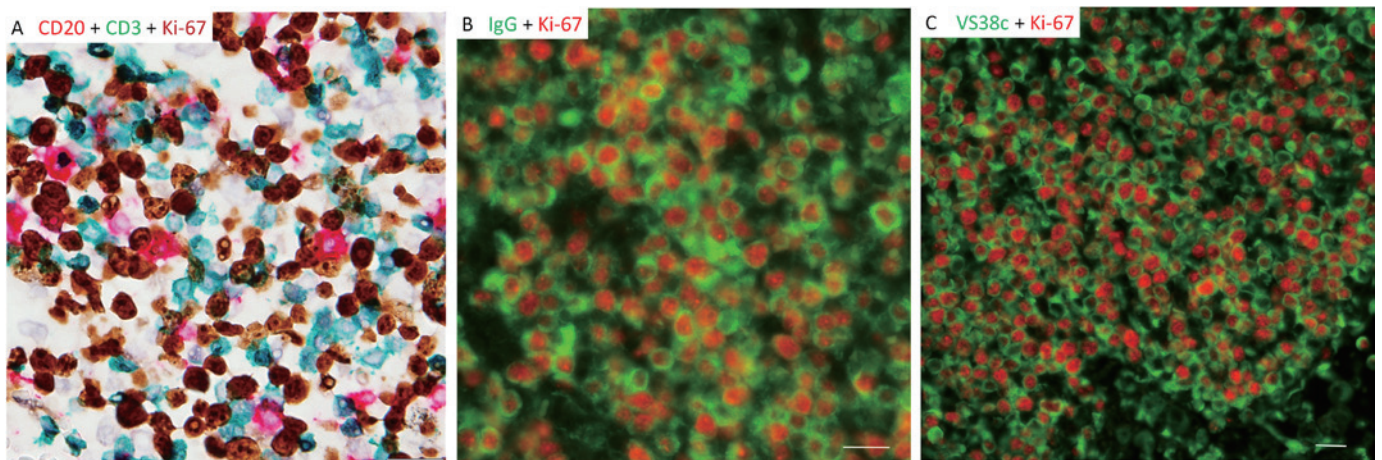


**Fig. 3.** Multi-labeling immunohistochemistry for phenotypic characterization of plasmablasts in the pulmonary hilar lymph nodes. *A*) Chromogenic method. Ki-67<sup>+</sup> cells (brown) did not correspond to CD20<sup>+</sup> (red) or CD3<sup>+</sup> (green) cells. *B*), *C*) Immunofluorescence method. Merged figures showing that IgG<sup>+</sup> cells (*B*, green) and VS38c<sup>+</sup> cells (*C*, green) were frequently double-positive for Ki-67 (red). Note that Ki-67 is positive in the nucleus (located in the center). Round cells in the extrafollicular areas were finally identified as plasmablasts. Scales: 20  $\mu$ m (*A-C*). Methods are described in the legends of Supplementary Figure 5.

retroperitoneal or mesenteric lymph nodes) were not abundant in IgG<sup>+</sup> Ki-67<sup>+</sup> cells (Fig. S5B), highlighting the peculiarity of lymph nodes in the pulmonary hilar and mediastinal regions. Plasmablasts were not detected in the liver (1,685 g), spleen (210 g), or bone marrow, and peripheral blood analysis did not demonstrate a significant number of plasmablasts. A true paracortex (T cell zone) with abundant CD3<sup>+</sup> T cells was located only beneath the surface area of the pulmonary hilar lymph nodes. Of note, some T cells in the paracortex co-expressed Ki-67 (Fig. S5C), suggesting the

presence of antigenic stimuli. Negative controls did not exhibit specific reactivity (Fig. S5D). No other inflammatory diseases or findings of viral infection were observed in other organs or tissues.

## DISCUSSION

We judged the pulmonary hilar and mediastinal lymph node pathology described above to be reactive lymphadenopathy with abundant plasmablasts.<sup>4,6</sup> Such cells are early

plasma cells that have proliferative and/or migratory activity. Of note, this usage of plasmablasts is different from the same term used for neoplasms (for example, plasmablastic lymphoma).<sup>8</sup> We demonstrated that double-labeling immunohistochemistry for immunoglobulin and Ki-67, in addition to VS38c and Ki-67, was useful to identify plasmablasts in tissue sections. The tissue preservation of lymph nodes in the present case was fairly good for an autopsy case, probably because ECMO was used until the terminal stage, which enabled us to apply the above double-staining technique and PCR analyses.

The present patient was 15 years old. More active immune responses may occur in lymph nodes in young patients than in older adults. However, a previous report on reactive lymphadenopathy in children did not describe a similar change.<sup>9</sup> Moreover, a report on lymphadenopathy associated with plasma cell responses did not describe cases similar to ours.<sup>10</sup> To our knowledge, lymph node lesions similar to those in our case, including childhood and adult cases, have not been reported.

The lesion we observed may have been caused by reactions by memory B lymphocytes, resulting in the rapid accumulation of IgG<sup>+</sup> (not IgM<sup>+</sup>) plasmablasts in the medullary cord of lymph nodes without *de novo* formation of germinal centers,<sup>11,12</sup> which was observed in our case. If the present lymphadenopathy was caused by a primary immune response, a mixture of IgM<sup>+</sup> and IgG<sup>+</sup> plasma cells, and proliferating B cells with the development of germinal centers should have been observed; however, such findings were absent in our case. The cause of the observed lymph node pathology remains unclear because no viruses were identified. However, the spatial relationship between the heart and the location of lymphadenopathy (only observed in the mediastinal areas) suggests that the lymphadenopathy was related to myocarditis.

One of the authors (HO) previously reported that the base of ulcerative colitis is abundant 'proliferating plasma cells'.<sup>13</sup> We (MM and HO) now consider the previously described 'proliferating plasma cells' to be plasmablasts for the following reasons: a) these round cells were immunohistochemically CD19<sup>+</sup> CD20<sup>-</sup> CD3<sup>-</sup> CD138<sup>+</sup> IgG<sup>+</sup> or IgA<sup>+</sup> (but IgM<sup>-</sup>), and b) CD19<sup>+</sup> or IgG<sup>+</sup> cells were frequently double-positive for Ki-67 (Table S2). Immunoelectron microscopy revealed that CD19<sup>+</sup> cells had well-developed rough endoplasmic reticulum, a feature consistent with antibody-secreting cells. In relation to this, flow cytometry revealed plasmablasts (*i.e.*, early plasma cells with migratory potential) in the peripheral blood of patients with ulcerative colitis.<sup>14</sup>

The present report described a case of plasmablast-rich, reactive lymphadenopathy. Further studies are required to clarify the significance of the lesion and the distribution of reactive plasmablasts in different inflammatory lesions. Our double-staining method for immunoglobulin and Ki-67 may be useful for this purpose.

## ACKNOWLEDGMENTS

We are grateful to Dr. Roderick E. Mitcham, Kindai University Faculty of Medicine, Japan, for critical reading of the manuscript. Technical assistance by Mr. Kakeru Sannomaru was greatly appreciated.

## INFORMED CONSENT

Written informed consent was received from the parents of the patient.

## AUTHOR CONTRIBUTIONS

HO performed all pathological analyses. MM interpreted the pathological data from the immunological viewpoint. YN, TM, LL, and JS treated the patient and summarized the clinical records. HO drafted the manuscript, and all authors participated in the discussion and completion of the manuscript.

## CONFLICT OF INTEREST

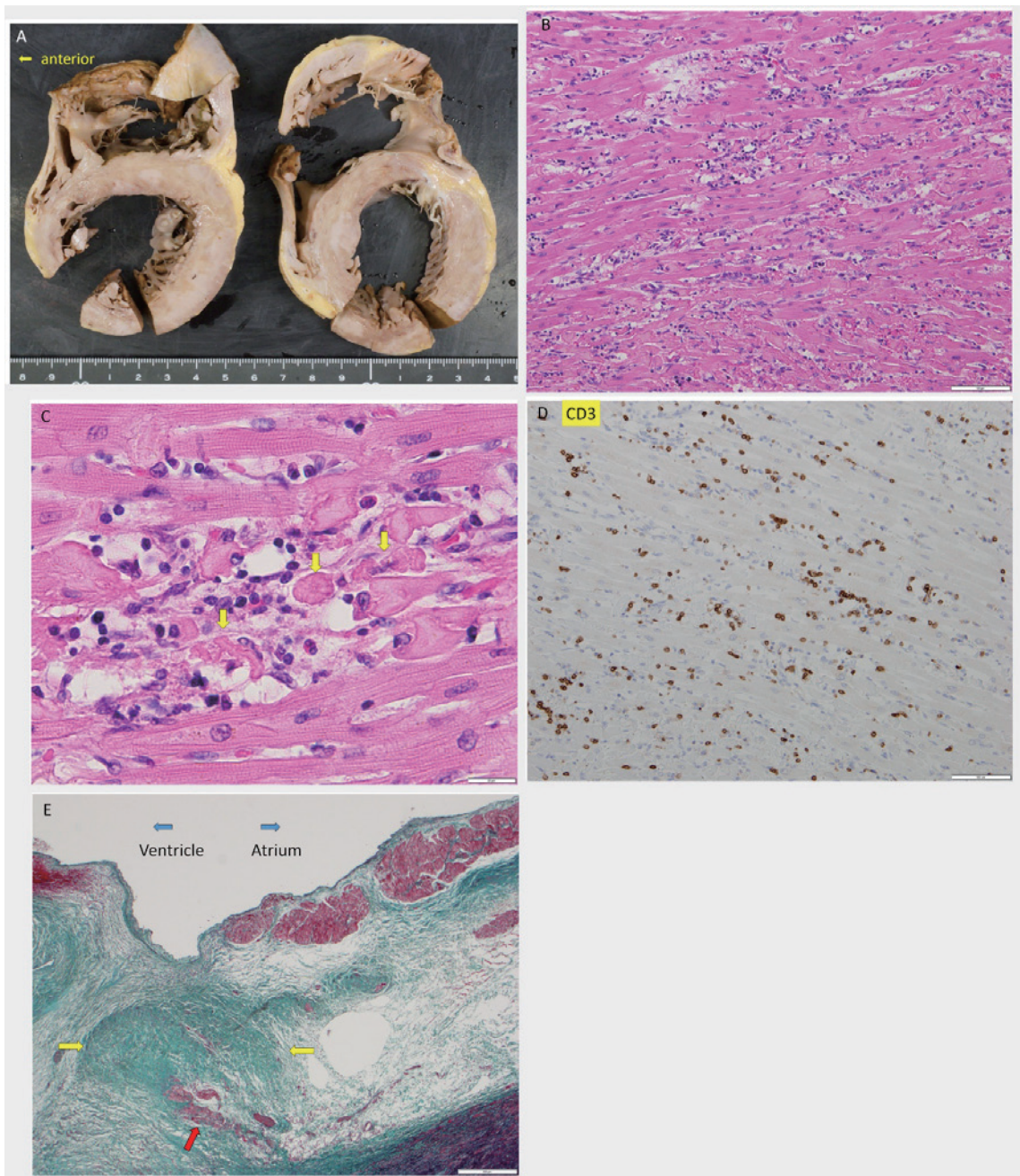
None declared.

## REFERENCES

- 1 Bracamonte-Baran W, Čiháková D. Cardiac Autoimmunity: Myocarditis. *Adv Exp Med Biol.* 2017; 1003 : 187-221.
- 2 Pollack A, Kontorovich AR, Fuster V, Dec GW. Viral myocarditis—diagnosis, treatment options, and current controversies. *Nat Rev Cardiol.* 2015; 12 : 670-680.
- 3 Turley H, Jones M, Erber W, *et al.* VS38: a new monoclonal antibody for detecting plasma cell differentiation in routine sections. *J Clin Pathol.* 1994; 47 : 418-422.
- 4 Nutt SL, Hodgkin PD, Tarlinton DM, Corcoran LM. The generation of antibody-secreting plasma cells. *Nat Rev Immunol.* 2015; 15 : 160-171.
- 5 Tellier J, Nutt SL. Plasma cells: The programming of an antibody-secreting machine. *Eur J Immunol.* 2019; 49 : 30-37.
- 6 Tarlinton D. Plasma cell biology. In : Honjo T, Reth M, Radbruch A, *et al.* (eds) : *Molecular Biology of B Cells*, 2nd ed, Cambridge, Academic Press, 2015; pp. 232-243.
- 7 van Dongen JJM, Langerak AW, Brüggemann M, *et al.* Design and standardization of PCR primers and protocols for detection of clonal immunoglobulin and T-cell receptor gene recombinations in suspect lymphoproliferations: Report of the BIOMED-2 Concerted Action BMH4-CT98-3936. *Leukemia.* 2003; 17 : 2257-2317.
- 8 Campo E, Stein H, Harris NL. Plasmablastic lymphoma. In : Swerdlow HS, Campo E, Harris NL, *et al.* (eds) : *WHO Classification of Tumours of Haematopoietic and Lymphoid Tissues*, Revised 4th ed, Lyon, IARC. 2017; pp. 321-322.
- 9 Ramsay AD. Reactive lymph nodes in pediatric practice. *Am J Clin Pathol.* 2004; 122(suppl) : S87-S97.
- 10 Xie Y, Vallangeon B, Liu X, Lagoo AS. Plasmacytic or lymphoplasmacytic infiltrate in lymph nodes: Diagnostic approach and

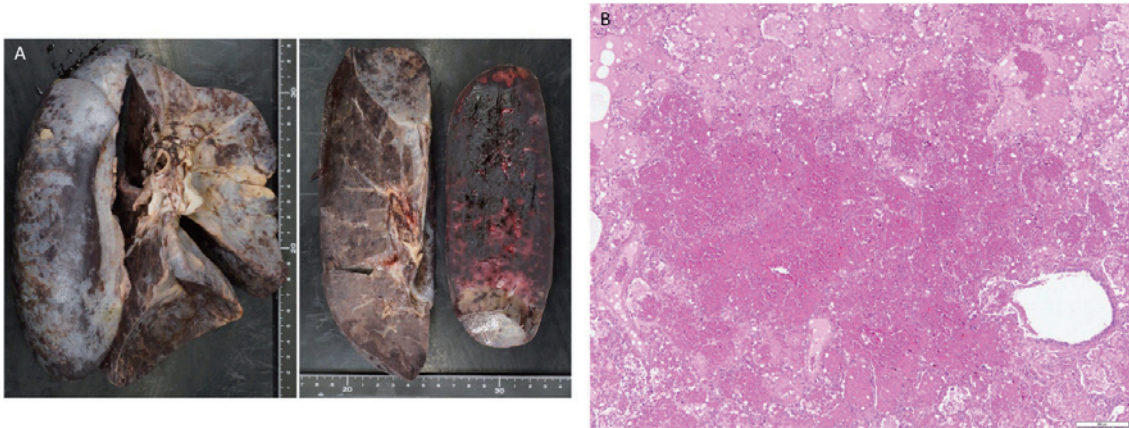
- differential considerations. *Indian J Pathol Microbiol.* 2016; 59 : 446-456.
- 11 Kurosaki T, Kometani K, Ise W. Memory B cells. *Nat Rev Immunol.* 2015; 15 : 149-159.
  - 12 Hoffman W, Lakkis FG, Chalasani G. B Cells, antibodies, and more. *Clin J Am Soc Nephrol.* 2016; 11 : 137-154.
  - 13 Jinno Y, Ohtani H, Nakamura S, *et al.* Infiltration of CD19+ plasma cells with frequent labeling of Ki-67 in corticosteroid-resistant active ulcerative colitis. *Virchows Arch.* 2006; 448 : 412-421.
  - 14 Tarlton NJ, Green CM, Lazarus NH, *et al.* Plasmablast frequency and trafficking receptor expression are altered in pediatric ulcerative colitis. *Inflamm Bowel Dis.* 2012; 18 : 2381-2391.

Supplementary Material

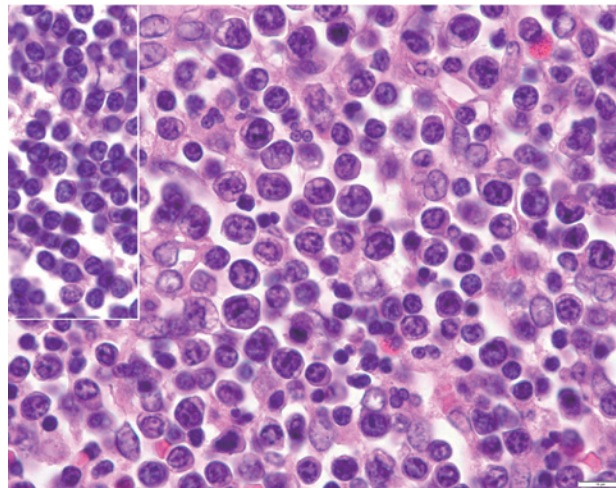


**Supplementary Fig. S1.** Autopsy findings of the heart.

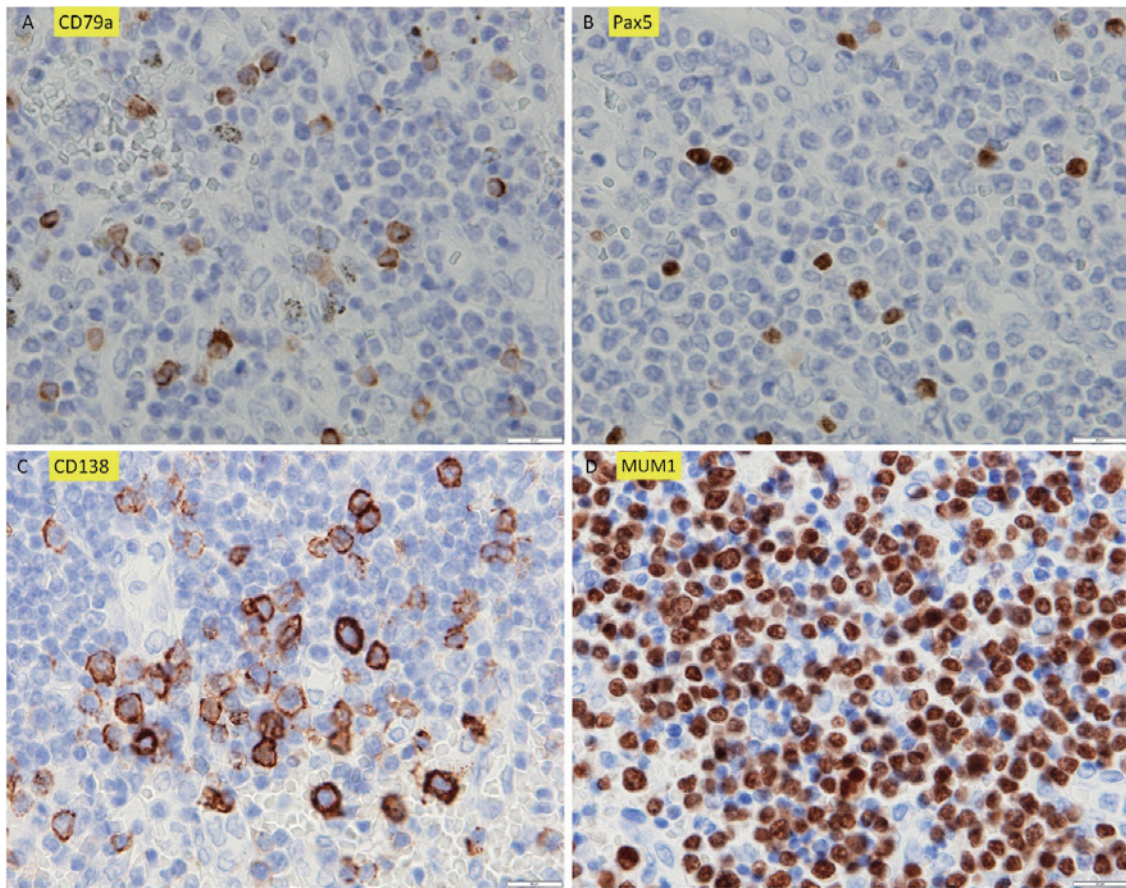
*A)* Macroscopic view of the myocardium (horizontal sections viewed from above) showed mild thinning of the myocardium of 9-10 mm in the left ventricle and 3 mm in the right ventricle. *B, C)* Microscopic findings of myocardial tissue (HE staining). Arrows in 1C indicate myocardial cell damage and/or necrosis. *D)* Immunohistochemistry for CD3 shows infiltration of myocardial tissue by CD3<sup>+</sup> T cells. *E)* Microscopic view of the atrioventricular (AV) node exhibiting scar formation (green) (yellow arrows). The red arrow indicates residual myocardial cells (brown color) in the AV node. Elastica-Masson/Goldner staining. This scarring corresponds to the previous acute myocarditis, demonstrating complete atrioventricular block, which later disappeared. Scales: 100  $\mu$ m (*B, D*), 20  $\mu$ m (*C*), and 500  $\mu$ m (*E*).



**Supplementary Fig. S2.** Autopsy findings of the lungs. *A*) Macroscopic findings of the right lung. The left lung showed the same findings. *B*) Microscopic findings of the lung, showing intra-alveolar hemorrhage and exudation of proteinaceous fluid (diffuse alveolar hemorrhage). Scale: 200  $\mu$ m (*B*).

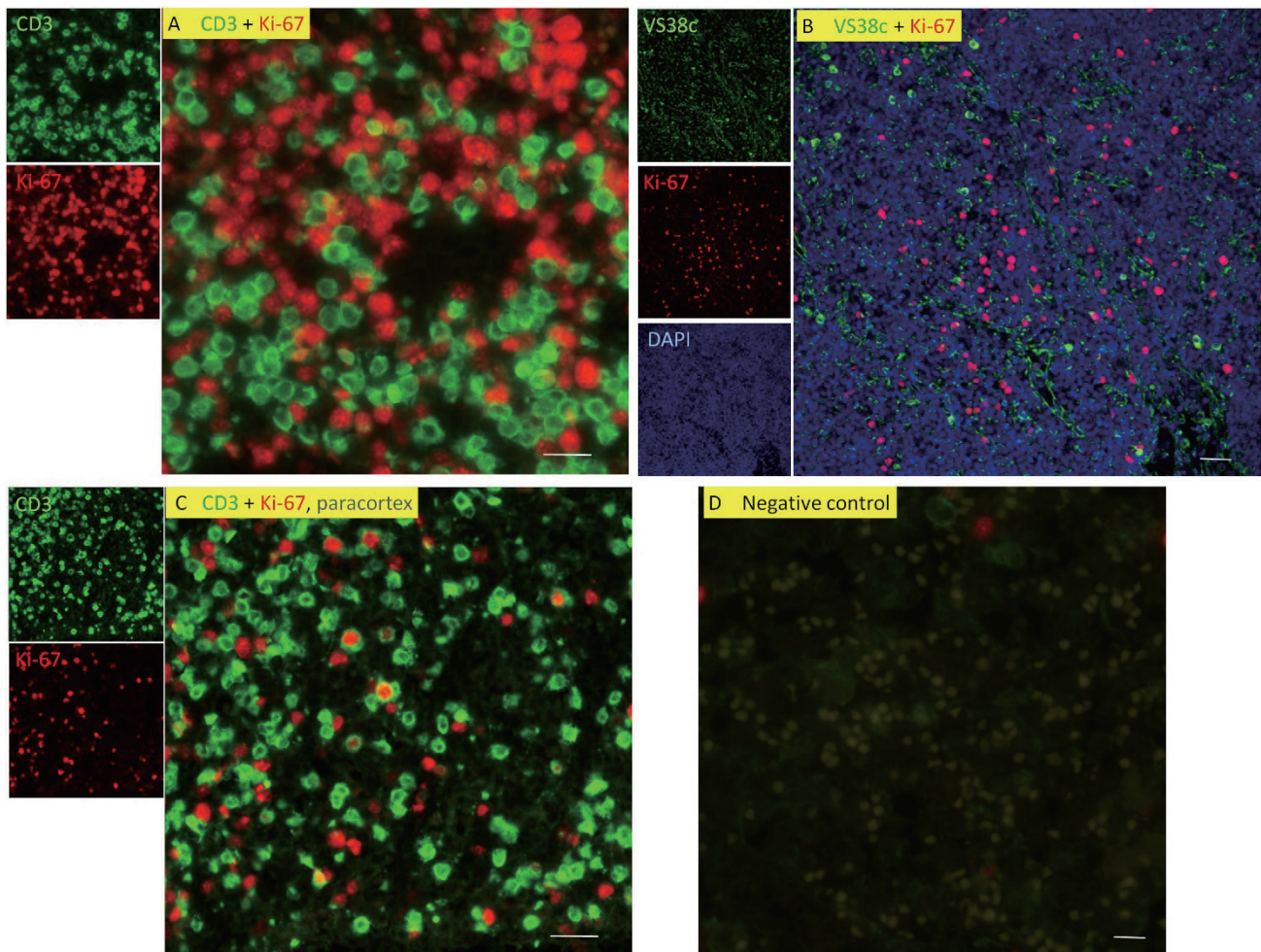


**Supplementary Fig. S3.** HE findings of plasmablasts. HE finding of plasmablasts filling the interfollicular areas of pulmonary hilar lymph nodes. Plasmablasts are round cells, some of which resemble plasma cells, but typical mature plasma cell morphology is hardly observable. Note that plasmablasts are larger (up to two-times) than the small lymphocytes observed in the left-upper inset at the same magnification. Scale: 10  $\mu$ m, the same for the inset.



**Supplementary Fig. S4.** Immunohistochemistry for plasmablasts. Immunohistochemistry for plasmablasts (reaction products shown in brown color). *A*) CD79a, *B*) Pax5, *C*) CD138, and *D*) MUM1. Most plasmablasts are negative for CD79a and Pax5, and positive for CD138 (up to 50% of the cells) and MUM1. Scale: 20  $\mu$ m (*A-D*).



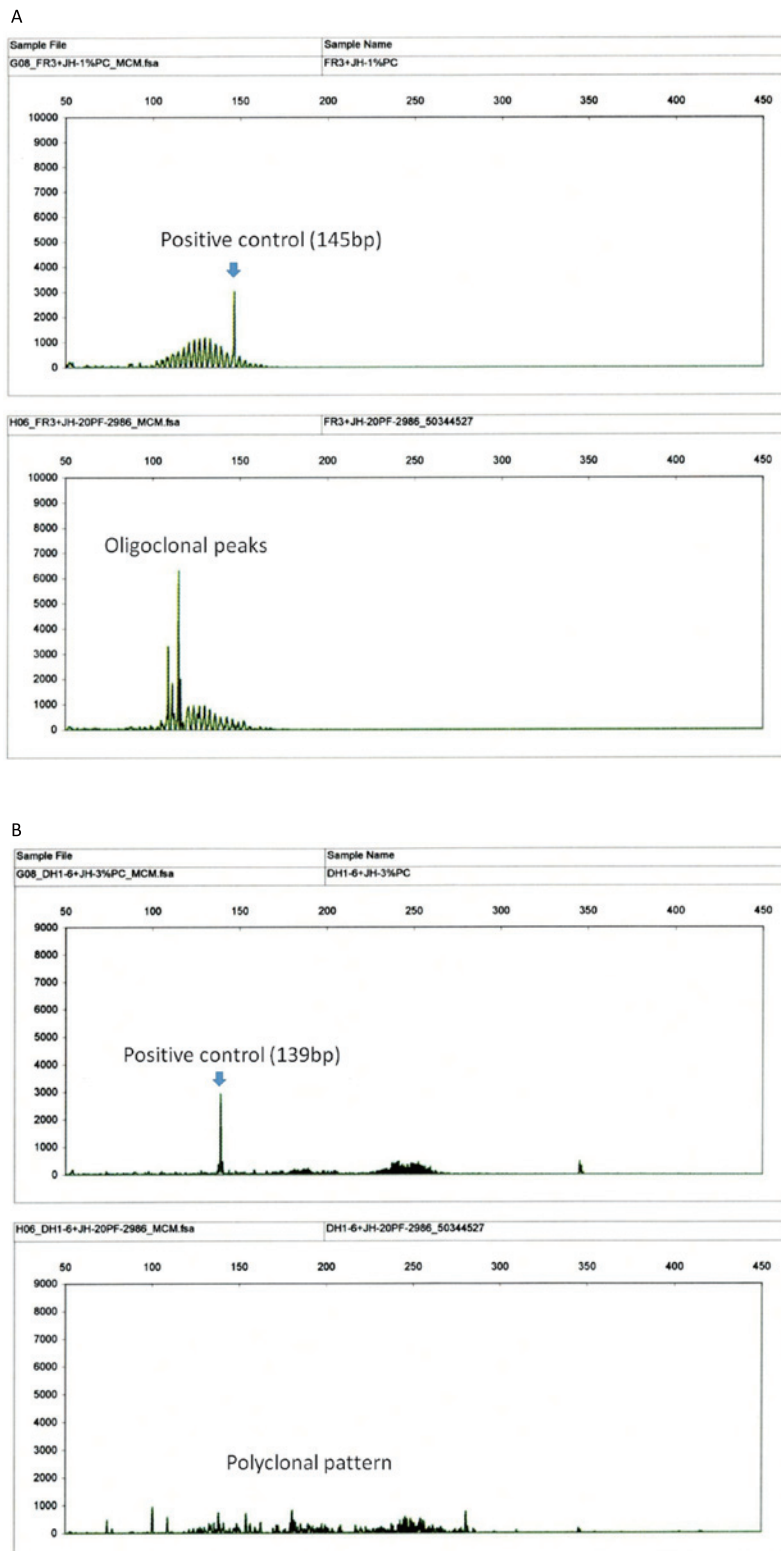


**Supplementary Fig. S5.** Double-labeling immunofluorescence microscopy.

Double-labeling immunofluorescence microscopy using formalin-fixed, paraffin embedded sections.

**A)** CD3<sup>+</sup> T cells did not show labeling of Ki-67 in the areas rich with plasmablasts in the pulmonary hilar node. **B)** VS38c<sup>+</sup> plasmablasts, few in number, did not show labeling of Ki-67 in the mesenteric lymph node. **C)** In the paracortex of pulmonary hilar lymph nodes, CD3<sup>+</sup> cells were occasionally double-positive for Ki-67. **D)** Negative control (the primary antibodies were omitted) demonstrated no specific reactivity. Scale: 20  $\mu$ m (**A-D**).

Methods: 1) Heat antigen retrieval (95C, 40 min, in pH 9 buffer), 2) anti-rabbit IgG (Leica Biosystems, Wetzlar, Germany) or mouse monoclonal VS38c antibody (DAKO/Agilent, Santa Clara, CA) for 30 min, 3) peroxidase block (Leica Biosystems) for 5 min, 4) secondary antibody (PerkinElmer, Waltham, MA), 30 min, 5) Opal (green, 1:150) (PerkinElmer) for 10 min, 6) heat treatment (95C, 10 min in pH 9 buffer), 7) anti-Ki-67 mouse monoclonal antibody (Leica Biosystems), 30 min, 8) Opal (red, 1:150), 10 min, 9) secondary antibody (PerkinElmer) for 30 min, 10) DAPI staining (PerkinElmer), 11) Aqueous mounting (ProLong Gold, ThermoFisher Scientific, Waltham, MA). The slides were observed on a Nikon E800 microscope equipped with band-pass filters (Nikon, Tokyo, Japan). The images were captured with a digital camera (DS-Ri2, Nikon) and merged (NIS-Elements software, Nikon). For negative controls, all primary antibodies were replaced with antibody-diluting solution (DAKO/Agilent).



**Supplementary Fig. S6.** Results of multiplex PCR analyses for immunoglobulin heavy chain variable region diversity. Genomic DNA was extracted from the formalin-fixed, paraffin-embedded sections of pulmonary hilar lymph nodes and diversity of the immunoglobulin heavy chain variable region was analyzed according to the standardized multiplex PCR protocol using the indicated primer set.

**A)**FR3-JH primer set

PCR using the FR3-JH primer set showed oligoclonal peaks and a polyclonal background.

**B)**DH1-6-JH primer set

PCR using the DH1-6-JH primer set yielded a polyclonal pattern.

No monoclonal peak was observed with FR1-JH, FR2-JH, or DH7-JH primer sets (not shown).

Data obtained at LSI Medience Corporation, Tokyo, Japan.

**Supplementary Table S1.** Virus analyses (data obtained during hospitalization)

(1) Present onset of myocarditis

real-time PCR				
	serum	plasma	pharynx	
enteroviruses (including coxsachievirus A/B, poliovirus, and echovirus)	not detected	not detected	not detected	
herpes simplex virus 1	not detected	not detected	(not done)	
herpes simplex virus 2	not detected	not detected	(not done)	
adenovirus	not detected	not detected	not detected	
influenza virus A/B	(not done)	(not done)	not detected**	
virus isolation				
	urine	stool	pharynx	
virus isolation	negative	negative	negative	
Antibodies to Epstein-Barr virus				
	EA IgG	VCA IgM	VCA IgG	EBNA IgG
Antibodies to Epstein-Barr virus	negative	negative	negative	negative

\*\* rapid antigen detection method

(2) Previous onset of myocarditis (3 years ago)

real-time PCR			
	serum	pharynx	
enteroviruses	not detected	not detected	
rotavirus type A	not detected	not detected	
adenovirus	not detected	not detected	
parvovirus 19	not detected	not detected	
virus isolation			
	urine	pharynx	sputum
virus isolation	negative	negative	negative

**Supplementary Table S2.** Pheno-types of plasmablasts

	HE	single-labeling immunohistochemistry								Ki-67 labeling index among IgG <sup>+</sup> cells
		CD19	CD20	CD79a	Pax5	CD138	VS38c	MUM1	Ig heavy chain	
The present case	round cells*	(+)	(-)	(-)	(-)	(+)	(+)	(+)	IgG	over 50%
Ulcerative colitis <sup>13</sup>	round cells**	(+)	(-)	n.d.	n.d.	(+)	n.d.	n.d.	IgG or IgA	over 50%

\* mature plasma cells hardly observed

\*\* mature plasma cells intermingled